

## Research Paper

# Structure in Dehydrated Trehalose Dihydrate—Evaluation of the Concept of Partial Crystallinity

Meena Rani,<sup>1,2</sup> Ramprakash Govindarajan,<sup>1</sup> Rahul Surana,<sup>1,3</sup> and Raj Suryanarayanan<sup>1,4</sup>

Received January 16, 2006; accepted May 8, 2006; published online August 23, 2006

**Purpose.** (i) To use trehalose as a model compound to evaluate the concept of crystallinity in pharmaceuticals. (ii) To understand the structural nature of dehydrated trehalose dihydrate.

**Materials and Methods.** Trehalose dihydrate was dehydrated isothermally at several temperatures below 100°C and the anhydrous product was characterized by XRD, DSC and water vapor sorption.

**Results.** XRD and DSC suggested that the dehydration product was a partially crystalline  $\alpha$ -polymorphic form of anhydrous trehalose ( $T_\alpha$ ). An increase in the temperature of dehydration resulted in a decrease in lattice order. In agreement with earlier findings, the ordered regions in the dehydrated lattice ( $T_\alpha$ ) converted to the dihydrate at much lower RH values than amorphous trehalose. However, the lattice order in the dehydrated product dictated the RH at which this conversion was initiated—the higher the lattice order the lower this RH. The structural nature of these samples can be explained based on the one-state model of crystallinity. In dehydrated trehalose, there is a continuum in lattice order ranging from highly crystalline  $T_\alpha$  to a completely disordered (i.e., amorphous) state.

**Conclusion.** The extent of lattice order in anhydrous trehalose ( $T_\alpha$ ) was dictated by the kinetics of water removal from trehalose dihydrate. The partially crystalline nature of anhydrous trehalose produced by dehydration could be described on a continuous scale of lattice order based on the one-state model of crystallinity.

**KEY WORDS:** amorphous; crystallinity model; dehydration; dihydrate; trehalose; water sorption;  $\alpha$ -polymorph.

## INTRODUCTION

The importance of physical characterization of pharmaceutical solids has long been recognized (1,2). The pharmaceutically relevant properties of active pharmaceutical ingredients (API) as well as excipients can be significantly influenced by their crystallinity. For example, while inadvertent surface amorphization by milling is known to affect processability, intentional amorphization of APIs has been utilized as an approach to improve bioavailability (3–5). Several analytical techniques used for the quantification of crystallinity, such as X-ray diffractometry, calorimetry, vapor sorption and spectroscopy, implicitly assume the *two-state model* of crystallinity. This model assumes that the lattice exists in either a completely ordered (100% crystalline) or a completely disordered (100% amorphous) state (6,7). The degree of crystallinity of a sample is expressed in terms of relative amounts of the two states in the sample. However,

lattice disorder generated during most pharmaceutical operations, e.g., milling, may be better described by the *one-state model* which assumes a gradual and continuous decrease in lattice order as we move from a perfectly ordered to a completely disordered lattice (6,7). When amorphization is induced by mechanical stresses during milling, lattice disordering is expected to occur preferentially in the surface regions of particles. This disruption can be visualized as a gradual increase in lattice order from the amorphous surface towards the crystalline core. In such systems, the extent of disorder in any given region of a solid may therefore be defined using this *continuous* one-state model. Most techniques used to quantify crystallinity are based on standard curves generated using mixtures of 100% crystalline and 100% amorphous “standards” (two-state model). The crystallinity of an unknown sample is determined from this standard curve based on the overall response of the sample. The calculated degree of crystallinity may therefore not reflect the nature of the disordered lattice.

Several pharmaceutical operations are known to generate disorder in solids. Processes such as freeze-drying and spray-drying of solutions often result in substantially amorphous products (8,9). On the other hand, lattice disorder can also be generated by mechanical processing of crystalline solids (4,5). The conditions of dehydration of hydrates can dictate the degree of crystallinity of the resulting anhydrate (10,11). Disordered solids obtained by different processes can

<sup>1</sup> Department of Pharmaceutics, University of Minnesota, 308 Harvard St. S.E., Minneapolis, Minnesota 55455, USA.

<sup>2</sup> Present address: Interpharm, Inc., 75 Adams Ave., Hauppauge, New York 11788, USA.

<sup>3</sup> Present address: Forest Laboratories Inc., 49 Mall Drive, Commack, New York 11725, USA.

<sup>4</sup> To whom correspondence should be addressed. (e-mail: surya001@umn.edu)

exhibit marked differences in their properties. In order to explain these differences, it may be necessary to understand the nature of the disorder.

Amorphization of trehalose, a disaccharide, for example can be brought about by freeze- or spray-drying of an aqueous trehalose solution, milling or melt quenching of the crystalline anhydrate and dehydration of trehalose dihydrate (12–14). The dehydration behavior of trehalose dihydrate ( $T_H$ ) has been of particular interest and has been extensively studied because of its possible relevance in desiccation tolerance of anhydrobiotic organisms (14–28). These studies have revealed the existence of several anhydrous polymorphic forms of trehalose. The formation of the  $\alpha$ - and the  $\beta$ - polymorphic forms,  $T_\alpha$  and  $T_\beta$  respectively, by dehydration of  $T_H$  was documented in 1962 (29). The effect of water vapor pressure on the dehydration product of  $T_H$  was recently evaluated. Non-isothermal dehydration under dry conditions yielded  $T_\alpha$ , while dehydration under conditions of high water vapor pressure (12 kPa) resulted in the stable  $\beta$ -form. At intermediate vapor pressures of 3 and 5 kPa, a new  $\epsilon$ -polymorph ( $T_\epsilon$ ) was obtained (17).

The formation and properties of  $T_\alpha$  have been the subject of detailed investigations (14,15,18–20,22,23,25,27,30).  $T_\alpha$  is formed by dehydration of  $T_H$  under dry conditions either isothermally at low temperatures (18,22,25,29) or when heated at low rates, where most of the dehydration is accomplished at low temperatures (14,15,19,20,27). However, under these conditions, the dehydration product was always a mixture of  $T_\alpha$  and amorphous trehalose ( $T_{am}$ ). As the rate of water removal decreased, the amorphous fraction in the product decreased. A supercritical  $CO_2$  extraction method was also evaluated for the efficient production of  $T_\alpha$  from  $T_H$  (30).  $T_\alpha$  is obtained at temperatures substantially less than the glass transition temperature ( $\sim 117^\circ C$ ) where the mobility is expected to be low. Hence, the  $T_\alpha$  structure was suggested to be a consequence of the nature of water departure from the lattice rather than the restructuring of the sugar framework (23,27). The structure of this form has been suggested to have a “topotactic” relationship with the parent hydrate (20,25). At lower rates of dehydration, the water is believed to leave the lattice by “hopping from site to site along channels that lead to the crystal surface” (23). This results in an open network in  $T_\alpha$  which has structural resemblance to  $T_H$  (25). It was also suggested that the passages for water molecules along the *c*-axis of the dihydrate were retained in the structure of  $T_\alpha$  (18). As a result, this crystalline phase converted more readily to the dihydrate than the amorphous ( $T_{am}$ ) or the stable  $T_\beta$  form (15,17,19). For example, while  $T_\alpha$  converted to  $T_H$  at a water vapor pressure of 2.1 kPa at  $35^\circ C$  (37% RH),  $T_\beta$  required a much higher vapor pressure of 6.2 kPa at  $40^\circ C$  (84% RH) (17). In another study, while amorphous trehalose did not convert to  $T_H$  at 43% RH ( $25^\circ C$ ),  $T_\alpha$  was found to convert within an hour (19).

The partially crystalline  $T_\alpha$  would be an excellent model system to evaluate the two concepts of crystallinity. As mentioned earlier, in  $T_\alpha - T_{am}$  mixtures,  $T_\alpha$  converted to  $T_H$  at lower RH values than  $T_{am}$ . According to the two-state model, the rehydration behavior of  $T_\alpha$ , produced under different conditions, should be the same. This is because the two-state model recognizes only two discrete states— crystalline and amorphous. However, according to the one-state model, the

rehydration behavior (critical RH of hydrate formation) of  $T_\alpha$  would depend on the extent of order retained. This is because the extent of lattice collapse, which is influenced by the rate of water removal, would have a bearing on the degree of disorder and hence the ability of the residual structure to re-incorporate water into the lattice. The rehydration behavior of partially crystalline  $T_\alpha$ , prepared under different dehydration conditions, has not been investigated so far. Besides, all the studies discussed above have demonstrated the rapid hydrate formation of the  $T_\alpha$  phase at a single, relatively high RH value in the range of 37–43% (15,17,19).

We hypothesize that (i) the lattice disorder induced by dehydrating trehalose dihydrate can be explained by the one-state model of crystallinity, and (ii) the dehydration conditions not only influence the fraction of  $T_\alpha$  in the product, but also the rehydration behavior of  $T_\alpha$ . Our objectives are: (i) to study the effect of temperature of dehydration of  $T_H$  on the structural nature of the anhydrous product, and (ii) to use dehydrated trehalose as a model system to evaluate the concept of partial crystallinity in pharmaceuticals.

## MATERIALS AND METHODS

### Materials

$\alpha$ ,  $\alpha$ -Trehalose ( $\alpha$ -D-glucopyranosyl  $\alpha$ -D-glucopyranoside) dihydrate ( $T_H$ ,  $C_{12}H_{22}O_{11} \cdot 2H_2O$ , Sigma, St. Louis, MO) was used as obtained. Crystalline  $\beta$ -trehalose ( $T_\beta$ ) was prepared by exposing  $T_H$  to 20% RH at  $60^\circ C$  for several hours.

### Preparation and *in Situ* Thermal Characterization of Anhydrous Trehalose

A differential scanning calorimeter (MDSC, Model 2920, TA Instruments, New Castle, DE) with a refrigerated cooling accessory was used. The instrument was calibrated with pure samples of tin and indium. About 5 mg of  $T_H$  was weighed in open aluminum pans, placed in the preheated DSC cell, and dehydrated isothermally under dry nitrogen purge (flow rate 70 ml/min unless otherwise stated). The dehydration temperatures were 40, 60, 85 or  $100^\circ C$ . The time required for dehydration decreased with an increase in the temperature ( $\sim 15$  min at  $100^\circ C$  to  $\sim 7$  h at  $40^\circ C$ ). Following dehydration, the sample was cooled to  $25^\circ C$  and either characterized immediately or stored at  $\sim 0\%$  RH under ambient temperature conditions until analysis. Thermal analysis was performed using open DSC pans at a heating rate of  $10^\circ C/min$  (results shown in Table I). Specific experimental details, wherever necessary, are provided in the Results and Discussion section.

### Preparation of the Amorphous Trehalose ( $T_{am}$ ) by Freeze-Drying

Aqueous trehalose solution (10% w/v) was cooled to  $-45^\circ C$  in a tray freeze-drier (Model UNITOP 400L, Virtis) and primary-dried for 48 h. Over the next 24 h, the temperature was gradually increased to  $50^\circ C$ . The secondary drying was carried out at  $50^\circ C$  for 24 h, after which the

**Table I.** Temperature of Melting of  $T_\alpha$  and its Enthalpy of Fusion ( $\Delta H_f$ ) as a Function of the Preparation Method (Temperature of Dehydration). The temperature of recrystallization of the  $\beta$ -form ( $T_\beta$ ) has also been reported

Dehydration temperature (°C)	Melting temperature of $T_\alpha$ (°C)		$\Delta H_f$ (J/g)	Recrystallization temperature of $T_\beta$ (°C) <sup>a</sup>
	Onset	Peak		
40	123.7 ± 0.8	132.4 ± 0.3	20.6 ± 0.9	203.6 ± 0.4
60	123.5 ± 0.1	130.8 ± 0.0	16.9 ± 0.5	203.0 ± 0.7
85	ND	129.5 ± 0.2	8.0 ± 0.6	201.8 ± 1.2
100	ND	130.2 ± 0.4	0.7 ± 0.4	203.6 ± 0.5

<sup>a</sup> Peak temperature.

ND: Not determined (due to overlapping glass transition event).

temperature was raised to 60°C and the drying continued for 24 more hours. The samples were removed from the freeze-drier and stored in a desiccator at room temperature over anhydrous calcium sulfate (RH ~0%) until used. The residual water content was <0.2% w/w (by Karl Fischer titrimetry). The samples were then handled in a controlled humidity environment (<5% RH, in a glove box) under ambient temperature conditions.

### Water Vapor Sorption

About 5–6 mg of the sample was placed in the sample pan of an automated moisture balance (DVS-1000, Surface Measurements Systems, London, UK). As a pre-conditioning step, the sample was dried under dry nitrogen flow (~0% RH) at 40°C for ~3 h. The water uptake was quantified over a range of RH values at 25°C. A small sample size coupled with prolonged equilibration time ensured equilibrium at each RH. The microbalance was calibrated using a 100 mg standard weight. The relative humidity sensor was calibrated at 5.0, 11.3, 32.8, 52.8, 75.3 and 84.3% RH (25°C), using saturated salt solutions. More specific details, wherever necessary, are provided in the [Results and Discussion](#) section.

### X-Ray Powder Diffractometry (XRD)

#### (a) Ambient Conditions

About 20 mg of sample was filled in a shallow quartz holder and exposed to  $\text{CuK}\alpha$  radiation (45 kV × 40 mA) in a wide-angle X-ray diffractometer (Model D5005, Siemens, Madison, WI). The instrument was operated in the step-scan mode, in increments of  $0.05^\circ 2\theta$ . The angular range was 5 to  $40^\circ 2\theta$ , and counts were accumulated for 1 s at each step. The data collection and analyses were performed with commercially available software (JADE, version 5.1, Materials Data, Inc., Livermore, CA).

#### (b) Controlled Environment

An X-ray powder diffractometer (Model XDS 2000, Scintag, Cupertino, CA) with a variable temperature stage (Model 828D, Micristar, R.G. Hansen and Associates, Santa Barbara, CA) was used to control the sample temperature. Water vapor pressure control was obtained using a previously

described assembly wherein a flow rate of 200 ml/min was used (31). About 10 mg of the sample was placed on the back of a copper holder and exposed to  $\text{CuK}\alpha$  radiation (45 kV × 40 mA) in the continuous mode at step increments of  $0.05^\circ 2\theta$ . The angular range was 5 to  $40^\circ 2\theta$  and the scanning rate was  $3^\circ 2\theta/\text{min}$ . During the XRD run, the sample was maintained under isothermal conditions.

## RESULTS AND DISCUSSION

### Characterization of Trehalose Dihydrate

XRD pattern of the  $T_H$  sample (Fig. 1a) was in excellent agreement with the published powder patterns of  $T_H$  (17,26). The DSC curve of  $T_H$  was characterized by a broad endotherm over the temperature range of 60 to 120°C due to dehydration followed by vaporization of water (not shown). This was followed by an endotherm at  $\sim 214^\circ\text{C}$  (peak), attributed to the melting of  $T_\beta$ . Dehydration under dry nitrogen flow in the vapor sorption balance resulted in a weight loss of ~9.5%, consistent with the stoichiometric water content of  $T_H$ .

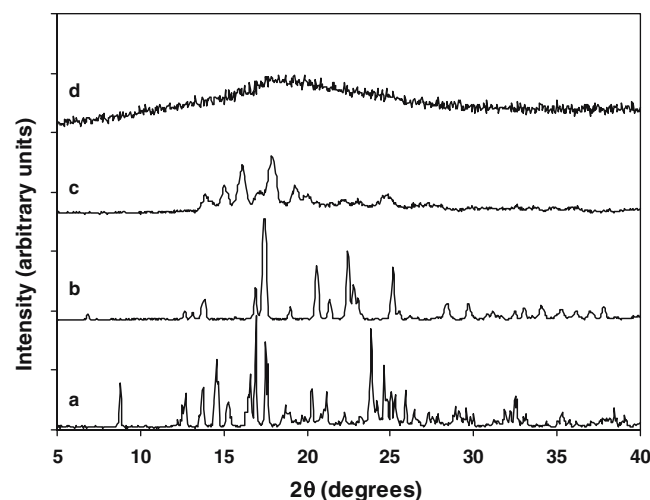


**Fig. 1.** Overlaid XRD patterns of (a) trehalose dihydrate ( $T_H$ ) (b)  $\beta$ -polymorph of anhydrous trehalose ( $T_\beta$ ), (c) anhydrous phase obtained by isothermal dehydration at  $40^\circ\text{C}$  ( $T_{40}$ ), and (d) freeze-dried trehalose ( $T_{am}$ ).

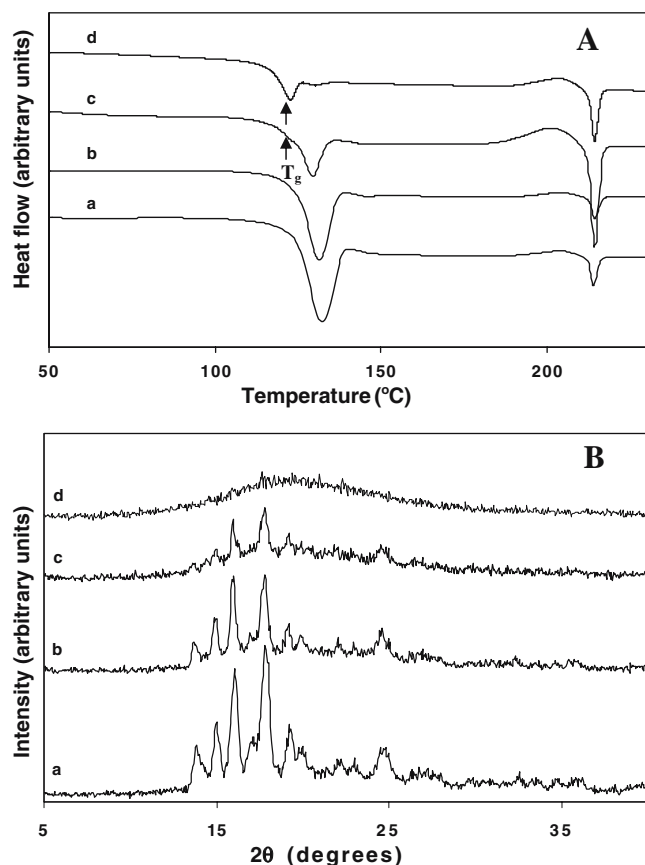


**Fig. 2.** (A) DSC profiles (panel A) and XRD patterns (panel B) of anhydrous trehalose obtained by isothermal dehydration of trehalose dihydrate at different temperatures; (a) 40°C (T<sub>40</sub>), (b) 60°C (T<sub>60</sub>), (c) 85°C (T<sub>85</sub>), and (d) 100°C (T<sub>100</sub>).

### Isothermal Dehydration of Trehalose Dihydrate at 40°C

T<sub>H</sub> was dehydrated isothermally for ~7 h at 40°C under dry nitrogen purge in an open DSC pan. The DSC heating curve (Fig. 2A, curve 'a') revealed an endotherm at ~131°C (peak), followed by an exotherm at ~203°C (peak) and an endotherm at ~214°C (peak). The first endotherm, with an onset temperature at 124°C, corresponds to the melting of T<sub>α</sub>, which is very close to the glass transition temperature of T<sub>am</sub>. A similar endothermic transition in T<sub>H</sub> samples dehydrated at 70°C under vacuum was attributed by Ding *et al.* to either the enthalpic recovery associated with glass transition of amorphous trehalose or to melting of residual pockets of the dihydrate (16). This event was later proved to be the melting of T<sub>α</sub> (14,25). The enthalpy of this transition (~21 J/g, Fig. 2A, curve 'a') was higher than the enthalpic recovery of amorphous trehalose following prolonged aging (32), but was considerably lower than the melting enthalpy of T<sub>β</sub> (14,25).

The X-ray pattern of the sample dehydrated at 40°C (Fig. 1c) matched closely with that of the α-polymorph obtained by dehydration of T<sub>H</sub> at slow heating rates of 0.5 to 1°C/min and exhibited characteristic peaks at 16.1° and 19.3°2θ (14,19,25). The broad amorphous halo in the XRD pattern (~10 to 30°2θ) also suggested amorphous character in the sample. For comparison purposes, XRD patterns of T<sub>H</sub>, T<sub>β</sub> and T<sub>am</sub> are also provided (Fig. 1).

### Effect of Dehydration Temperature on Solid-State of the Product

The rapid dehydration of trehalose dihydrate at 100°C is known to produce vitrified trehalose (12). Since dehydration at 40°C resulted in a material with substantial lattice periodicity, it was of interest to study the effect of the dehydration temperature on the solid-state of the dehydration product. Trehalose dihydrate was therefore isothermally dehydrated in the DSC at 40, 60, 85 and 100°C under N<sub>2</sub> flow (hereafter these samples are referred to as T<sub>40</sub>, T<sub>60</sub>, T<sub>85</sub> and T<sub>100</sub>, respectively). The DSC heating profiles obtained by heating the dehydrated samples at 10°C/min, are presented in Fig. 2A. With an increase in the dehydration temperature, the enthalpy of the T<sub>α</sub> melting endotherm (onset ~125°C) decreased (Fig. 2A). While only one endotherm was observed for T<sub>40</sub> and T<sub>60</sub>, T<sub>85</sub> exhibited two overlapping endotherms where the lower temperature endotherm could be seen as a shoulder. For T<sub>100</sub>, T<sub>α</sub> melting endotherm was very weak and a small endotherm at ~118°C was also observed. Thus, dehydration at 40°C predominantly led to the formation of the most crystalline T<sub>α</sub>. Increase in dehydration temperatures resulted in decreased lattice order in the product.

Due to low crystallinity of T<sub>85</sub>, the glass transition was observed as a shoulder on the low temperature side of the T<sub>α</sub> melting endotherm (Fig. 2A, curve 'c'). Dehydration at 100°C resulted in almost completely amorphous trehalose, wherein the first endotherm with onset at 118°C could be attributed to enthalpic recovery that was followed by the weak T<sub>α</sub> melting endotherm (Fig. 2A, curve 'd'). In the samples dehydrated at 40 or at 60°C, the pronounced T<sub>α</sub> melting endotherm is likely to mask the glass transition event. Though the thermal behavior in the temperature range of 100 to 140°C depended on the method of preparation of anhydrous trehalose (Fig. 2A), in every case, crystallization of T<sub>β</sub> was observed at ~200°C which subsequently melted at ~214°C (exotherm followed by endotherm).

The above results were confirmed by XRD of the isothermally dehydrated samples (Fig. 2B). The intensity of the characteristic peaks of T<sub>α</sub> decreased with an increase in the dehydration temperature. The presence of an amorphous halo and absence of peaks of any other form of trehalose in the XRD patterns suggested that dehydration resulted in a mixture of T<sub>α</sub> and T<sub>am</sub>. In line with the DSC results, the phase obtained by dehydration at 100°C was characterized predominantly by an amorphous halo. While there is a decrease in crystallinity with an increase in dehydration temperature, it is not possible to conclude whether the dehydrated product is a simple mixture of two phases (highly ordered T<sub>α</sub> and amorphous anhydrate) or there is a continuum in the lattice order.

### Quantification of T<sub>α</sub>

Our next objective was to quantify the T<sub>α</sub> content in the anhydrous trehalose prepared under different conditions. XRD was used for this purpose. Since all the samples were partially X-ray crystalline, it was first necessary to separate the crystalline (I<sub>c</sub>) and amorphous (I<sub>a</sub>) intensities in each powder pattern. The crystallinity (T<sub>α</sub> content) was estimated



**Table II.** Quantification by XRD and DSC of the  $T_{\alpha}$  Content in Anhydrous Trehalose

Dehydration Temp (°C)	Determined by XRD		Determined by DSC	
	Percent crystallinity <sup>a</sup>		Enthalpy of fusion (J/g) <sup>b</sup>	Percent crystallinity
40	62		20.6 ± 0.9	61
60	52		16.9 ± 0.5	50
85	29		8.0 ± 0.6	24

The anhydrous trehalose was prepared by dehydration of trehalose dihydrate at different temperatures.

<sup>a</sup> Determined using Eq. (1);  $n = 2$ .

<sup>b</sup> Assuming the enthalpy of fusion of 100% crystalline  $T_{\alpha}$  is 33.9 J/g;  $n \geq 3$ .

by simplifying the method developed by Hermans and Weidinger (33). The degree of crystallinity ( $x_{cr}$ ) is expressed by the equation,

$$x_{cr} = \frac{I_c \times 100}{I_c + I_a} \quad (1)$$

A unique feature of this method is that the determination of the crystallinity of unknown samples requires neither a crystalline nor an amorphous standard. The  $I_a$  and  $I_c$  values were obtained over the angular range of 13 to 21°2 $\theta$  from which the  $T_{\alpha}$  content was determined (Table II). It is evident that, irrespective of the dehydration temperature, the anhydrous trehalose was only partially crystalline in the temperature range of 40 to 85°C. In this context, it has been reported that the  $T_{\alpha}$  form does not exhibit preferred orientation. In fact, a  $T_H \rightarrow T_{\alpha} \rightarrow T_H$  transformation was shown to remove the preferred orientation in the sample (19).

The degree of crystallinity can also be determined by DSC, wherein the ratio of the enthalpy of fusion of the unknown sample to that of the 100% crystalline standard forms the basis for quantification. However, our inability to prepare a 100% crystalline standard of  $T_{\alpha}$ , posed a problem. The enthalpy of fusion of highly crystalline  $T_{\alpha}$  was reported to be 33.9 J/g (11.6 kJ/mole) (14). In the quantification of crystallinity, this value was used as the enthalpy of fusion of 100% crystalline  $T_{\alpha}$ . As is evident from Table II, the DSC and XRD estimates are in reasonably good agreement.

### Effect of Nitrogen Flow Rate on the Solid-State of the Dehydrated Product

The dehydration experiments, carried out at different temperatures, indicated that the rate of water removal influenced the physical form of the anhydrous phase formed, which is in agreement with existing reports (27). While slow dehydration tends to facilitate formation of  $T_{\alpha}$ , rapid water removal resulted in a collapsed lattice. It is well known that the kinetics of water removal can influence the physical state of the anhydrous phase obtained (12,27). In order to investigate this issue, the nitrogen flow rate during dehydration was varied while maintaining the temperature constant. The experiments were carried out at 40 and at 85°C, and at flow rates of 0, 40 and 70 ml/min. Following the dehydration, the sample was subjected to DSC and the enthalpy of fusion of the anhydrous  $T_{\alpha}$  (peak at 131°C), provided a measure of the crystalline fraction (Table III). When the dehydration was carried out at 40°C, decreasing the flow rate from 70 to 0 ml/min, resulted in an increase in the  $T_{\alpha}$  content from ~60 to ~80%. Interestingly, at 85°C, the flow rate did not influence the composition of the anhydrous phase. Thus, the nitrogen flow influenced the phase composition only at a low dehydration temperature.

At 85°C, irrespective of the nitrogen flow rate, rapid dehydration is expected to be followed by instantaneous water removal. Thus the nitrogen flow rate is unlikely to influence the dehydration and vaporization kinetics. However, at the lower temperature of 40°C, because of the low vapor pressure of water, the flow rate will have a pronounced

**Table III.** Effect of Nitrogen Flow Rate on the Melting Temperature and the Enthalpy of Fusion of  $T_{\alpha}$ 

Dehydration Temp. (°C)	Nitrogen flow rate (ml/min)	Melting temperature of $T_{\alpha}$ (°C)		Enthalpy of fusion (J/g)	Crystallization temperature of (°C) <sup>a</sup>	Percent crystallinity
		Onset	Peak			
40	70	123.8	131.9	20.6 ± 0.9	203.6 ± 0.4	61
40	40	123.7	131.9	23.8	202.8	70
40	0	123.9	130.7	26.9	203.1	79
85	70	124.5	131.4	8.0 ± 0.6	201.8 ± 1.2	24
85	40	123.9	129.7	8.9	202.2	26
85	0	124.7	130.2	8.4	202.6	25

The temperature of crystallization of  $T_{\beta}$  has also been reported. The anhydrous trehalose was prepared by dehydration of trehalose dihydrate at different temperatures and nitrogen flow rates.

<sup>a</sup> Peak temperature.

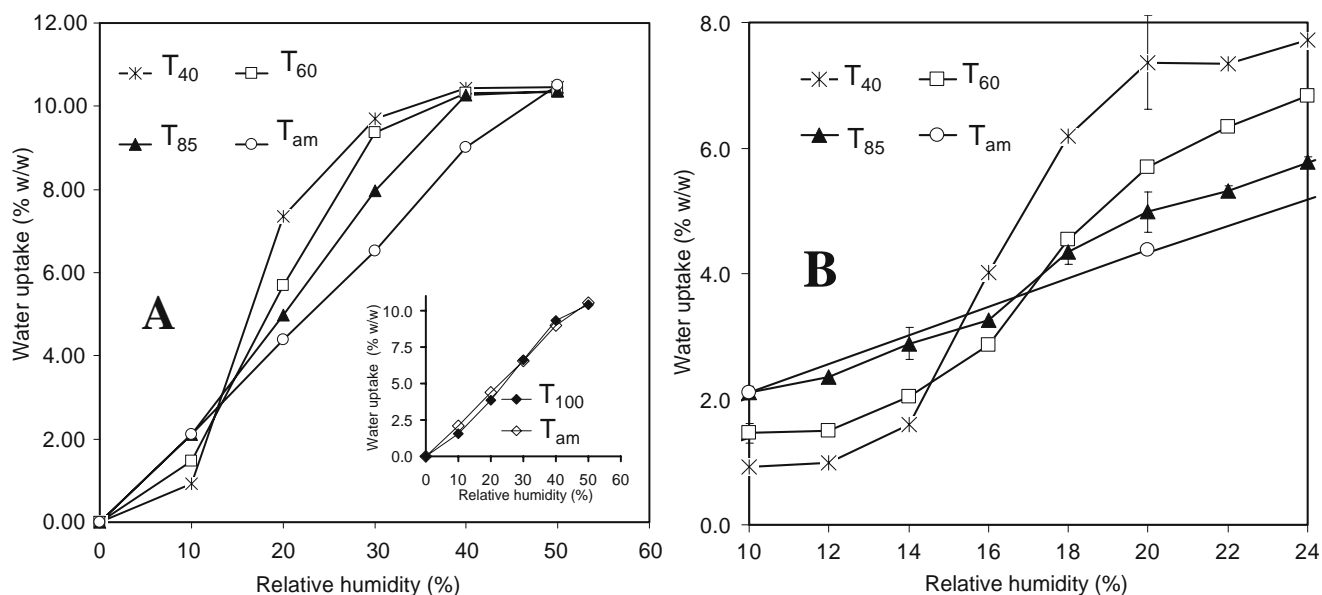


**Fig. 3.** (A) The water uptake behavior of T<sub>40</sub>, T<sub>60</sub> and T<sub>85</sub> at 25°C. The water uptake behavior of T<sub>am</sub> has been overlaid for comparison. Inset: Comparison of water uptake profile of T<sub>100</sub> (X-ray amorphous sample) with T<sub>am</sub> at 25°C. (B) Comparison of the water uptake behavior, of the samples in the range of 10 to 24% RH.

influence on the kinetics of water vaporization. A high flow rate will facilitate the rapid removal of the water liberated by dehydration, thus accelerating the overall dehydration reaction. This in turn will favor the formation of the amorphous anhydrate, reflected by the lower enthalpy of fusion (Table III). This confirms that the rate of water removal from the T<sub>H</sub> lattice is the major determinant of the extent of lattice order retained in the product phase.

### Water Uptake by the Dehydrated Product

The water uptake behavior of the isothermally dehydrated samples was studied at 25°C in the RH range of 0–50% (Fig. 3A). For the sake of comparison, the water uptake behavior of the amorphous freeze-dried sample is also shown. At 25°C, trehalose dihydrate is the stable form at RH  $\geq$  50%. The dehydration temperature had a pronounced influence on the water uptake behavior of the resulting anhydrate. When exposed to 10% RH, T<sub>40</sub> exhibited the lowest water sorption. Freeze-dried trehalose sorbed the maximum amount of water. This is consistent with our observation that the lower the temperature of dehydration, more ordered is the dehydration product, with a consequent decrease in the amount of water sorbed (Table II, Fig. 3A). Interestingly, this trend was reversed at higher RH values of 20 and 30% (Fig. 3A). All the samples were expected to convert to trehalose dihydrate at RH  $\geq$  50%. Thus, based on conventional wisdom, at any RH up to 50%, since amorphous trehalose was expected to sorb more water than T <sub>$\alpha$</sub> , maximum water uptake was expected in freeze-dried trehalose. However, the above belief holds true only at 10% RH (Fig. 3A, main figure). These observations could be explained by humidity-controlled XRD.

When T<sub>40</sub> was exposed to 5 and 10% RH, the water uptake did not result in any detectable phase transition by XRD (Fig. 4). On the other hand, when it was exposed to 20% RH, the characteristic peaks of trehalose dihydrate

(e.g., 8.8, 12.7 and 23.9°2 $\theta$ ) were observed. It is also well documented in the literature that, at 25°C, the transition: T<sub>am</sub>  $\rightarrow$  T<sub>H</sub> does not occur at RH up to 45% (12,32,34,35). Therefore, T <sub>$\alpha$</sub>  transforms to T<sub>H</sub> at a lower RH than T<sub>am</sub>. Let us compare the water sorption behavior of the four trehalose samples at 20% RH (Fig. 3A). The amorphous form prepared by freeze-drying only sorbs water, with no attendant phase transition to trehalose dihydrate. On the other

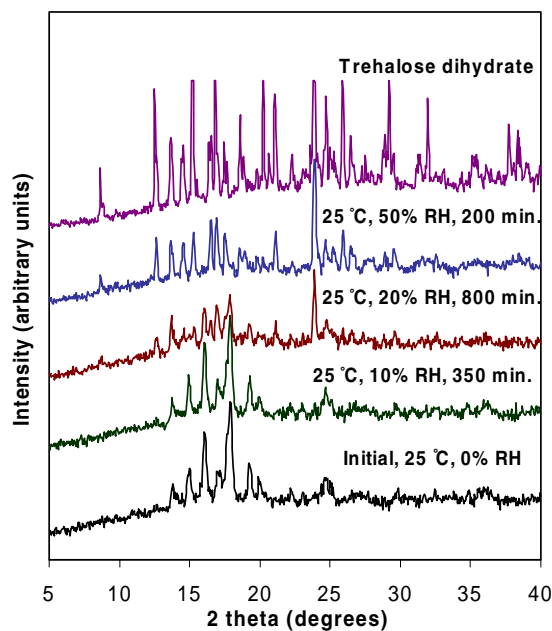


**Fig. 4.** Phase transitions in T<sub>40</sub> as a function of RH. The powder, placed in the sample chamber of an XRD, was subjected to progressively higher RH values. At each RH, XRD patterns were obtained periodically. When no further changes were observed, the RH was increased. The XRD pattern of trehalose dihydrate has been provided for comparison.

**Table IV.** Fraction of Anhydrous Trehalose Converted to Trehalose Dihydrate Following Storage at 20 and 30% RH (at 25°C)

Dehydration Temp. (°C)	Fraction converted to dihydrate (%)	
	20% RH	30% RH
40	37	74
60	22	71
85	10	36
Freeze-dried	0	0

The anhydrous trehalose was prepared by dehydrating trehalose dihydrate at 40, 60 or 85°C. For comparison purposes, the behavior of the freeze-dried amorphous trehalose is also provided.

hand, in case of the partially crystalline anhydrous form, while the amorphous component sorbs water, the crystalline component incorporates the water into the lattice to form the dihydrate. Thus, the higher the  $T_{\alpha}$  content in the anhydrous trehalose, the higher the trehalose dihydrate content following storage at 20% RH. Thus the sample prepared by dehydration at 40°C, which had the highest  $T_{\alpha}$  content (Table II), exhibited maximum water uptake and extent of conversion to dihydrate at 20% RH (Table IV; details to be discussed later).  $T_{85}$ , owing to its low  $T_{\alpha}$  content (Table II), showed the least conversion to the dihydrate following storage at 20% RH (Table IV). This unusual observation confirms the belief of a structural similarity between  $T_{\alpha}$  and  $T_H$  phases. Based on stoichiometric water uptake, the partially crystalline  $T_{\alpha}$ , prepared by isothermal dehydration at 40, 60 and 85°C *seem* to have transformed to  $T_H$  at 40% RH (water uptake of  $\sim 10.5\%$  w/w on anhydrous basis, Fig. 3A). However,  $T_{am}$  converted to the dihydrate only at 50% RH. The inset in Fig. 3A compares the water uptake profiles of two X-ray amorphous trehalose samples, one pre-

pared by freeze drying and the other by dehydration of  $T_H$  at 100°C. The sorption curves were very similar. However, the DSC curve of the sample dehydrated at 100°C revealed a small endotherm attributable to the melting of  $T_{\alpha}$  ( $\sim 0.3\%$  w/w  $T_{\alpha}$ ; Fig. 2A, curve 'd'). This and aging of the sample at high temperature (12,32), may explain the small differences in the water uptake behavior at low RH values (Fig. 3A, inset). It is therefore reasonable to assume that the water sorption behavior of the amorphous trehalose formed by dehydration of  $T_H$  is similar to freeze dried trehalose.

The anhydrous trehalose samples were subjected to 2% RH increments in the range of 10 to 24% so as to develop a more complete understanding of the water sorption behavior of trehalose (Fig. 3B). In the samples prepared by dehydration at 40, 60 and 85°C, there was a distinct step-change in the amount of water sorbed at 16, 18 and 18% RH, respectively. Above these RH values, the amount sorbed exceeded the uptake by the freeze-dried anhydrate, suggesting the first evidence of anhydrate  $\rightarrow$  dihydrate transition. As the RH was further increased, these samples progressively sorbed much more water than  $T_{am}$ . Based on water sorption data all the anhydrous samples prepared by dehydration had taken up water equivalent to the stoichiometric water content of the dihydrate at 40% RH.

The water sorption results suggest that the  $T_{\alpha} \rightarrow T_H$  conversion is not complete at a single RH value, but occurs over a range of RH values; this range is higher for samples with lower degree of lattice order. In order to confirm this, XRD patterns of  $T_{40}$  and  $T_{85}$  were recorded immediately after equilibration at 16, 20 and 30% RH (25°C). The powder pattern of  $T_{am}$  after equilibration at 30% RH served as a control (Fig. 5; panel H).  $T_{85}$  and  $T_{40}$  exhibited the characteristic peaks of  $T_{\alpha}$  at  $16.1$ ,  $17.9$  and  $19.3^{\circ}2\theta$  (panels A and E in Fig. 5). On exposure to 16% RH,  $T_{85}$  (panel B) did not

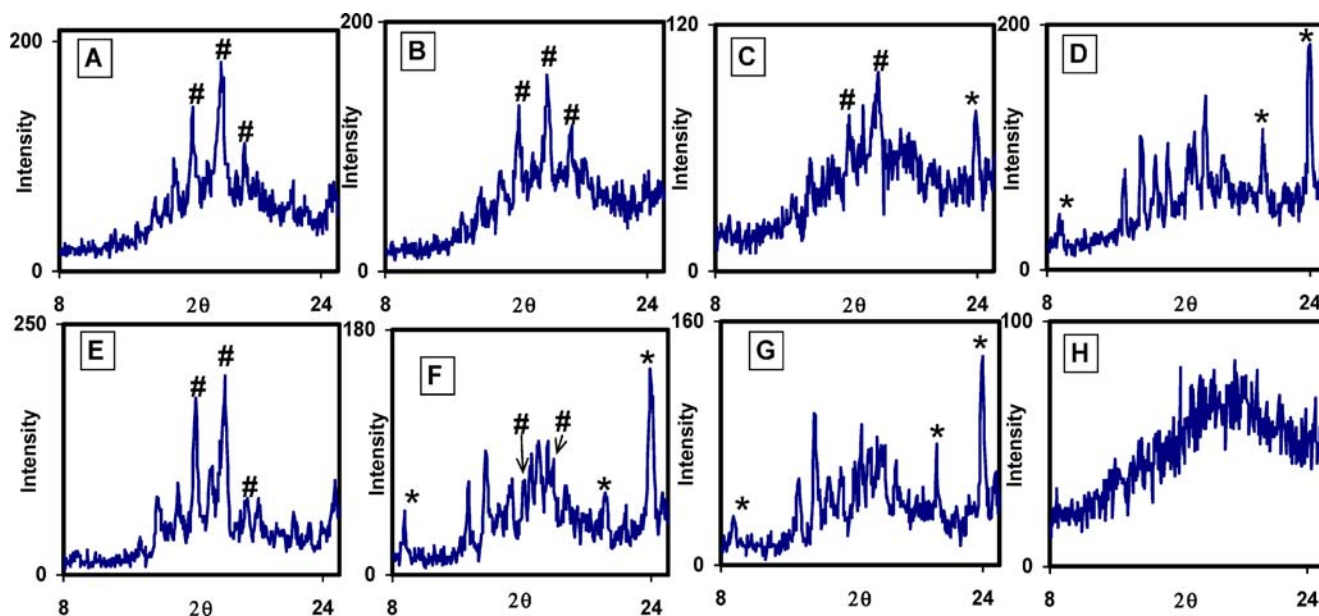


**Fig. 5.** Top row: XRD patterns of trehalose dihydrate ( $T_H$ ) dehydrated at 85°C and stored at 0% (panel A), 16% (panel B), 20% (panel C) and 30% RH (panel D). Bottom row: XRD patterns of trehalose dihydrate dehydrated at 40°C and stored at 0% (panel E), 16% (panel F), and 20% (panel G). The XRD pattern of freeze-dried amorphous trehalose equilibrated at 30% RH (panel H) is also provided for comparison. The samples B to D and F to H were equilibrated at the said RH values in the automated vapor sorption balance, removed and transported in sealed vials and their powder XRD patterns were recorded immediately. Characteristic  $T_H$  (\*) and  $T_{\alpha}$  (#) peaks have been marked.

show detectable conversion to  $T_H$ , while  $T_{40}$  (panel F) transformed to a substantial extent. This was seen as the appearance of the characteristic peaks of  $T_H$  at  $8.8$ ,  $21.1$  and  $23.9^\circ 2\theta$ . However, retention of the characteristic  $T_\alpha$  peaks indicates that the  $T_\alpha \rightarrow T_H$  transformation is not complete (panel F). Exposure of  $T_{40}$  to a higher RH of 20%, caused the disappearance of  $T_\alpha$  peaks suggesting conversion of highly ordered  $T_\alpha$  regions to  $T_H$  (panel G). On the other hand, the XRD pattern of  $T_{85}$  equilibrated at 20% RH revealed conversion of a fraction of  $T_\alpha$  to  $T_H$ . The peaks attributable to  $T_\alpha$  disappeared only when the RH was increased to 30% (panel D). The  $T_{am}$  remained amorphous even after exposure to 30% RH. It was reported that freeze-dried amorphous trehalose does not undergo any phase transformation even when stored at 45% RH (25°C) in spite of sorption of 10% w/w of water (35).

A comparison of the water uptake profiles of  $T_{40}$  and  $T_{85}$  at 16% RH (Fig. 6), reveals that  $T_{40}$  exhibited a biphasic profile, with an initial rapid uptake of  $\sim 1.5\%$  w/w water followed by a slow second phase. This was not seen with  $T_{85}$ . Both samples however exhibited similar water content when stored to a constant weight. It has been reported that in ' $T_{am}-T_\alpha$  mixtures,' the water is preferentially taken up by  $T_\alpha$  to form the dihydrate (19). The initial rapid water uptake in the sample with higher lattice order ( $T_{40}$ ) can therefore be attributed to  $T_H$  formation in the highly ordered regions in the lattice. The second stage may be attributed to water sorption into the disordered regions and  $T_H$  formation in the regions of lower lattice order.

It is readily apparent that lower the temperature of formation of trehalose anhydrate (i.e., dehydration temperature), the lower the RH where the anhydrate  $\rightarrow$  dihydrate transition is initiated. More importantly, the anhydrate  $\rightarrow$  dihydrate transition did not occur completely at a single RH value. In all the samples prepared by dehydration, there was a gradual and continuous anhydrate  $\rightarrow$  dihydrate transition which seemed to be complete by 40% RH. The RH at which

this transition was initiated, as mentioned earlier, varied between 16 and 20% RH.

As discussed earlier, if the samples prepared by dehydration were composed of distinct " $T_\alpha$ " and " $T_{am}$ " regions (i.e., two-state model of crystallinity), one would expect a fixed RH at which each of these phases would transform to the dihydrate. The observed progressive and gradual anhydrate  $\rightarrow$  dihydrate transition as a function of the RH suggests a continuous scale of lattice disorder as described by the one-state model. In order to confirm this, we attempted to estimate the  $T_\alpha$  content in the anhydrous trehalose based on the amount of water sorbed as a function of RH. This estimation assumes distinct ordered and disordered phases and was based on the following observations. (i)  $T_{am}$  did not transform to the dihydrate at RH  $< 45\%$ . (ii) Highly ordered  $T_\alpha$  converted to the dihydrate at RH  $\geq 20\%$ . Therefore, at  $20\% > RH > 45\%$ , any anhydrate  $\rightarrow$  dihydrate transformation can be attributed to  $T_\alpha$ . The water sorption was quantified at 20 and 30% RH (25°C). In the anhydrous trehalose, if the weight fraction of amorphous trehalose is  $x$ , the  $T_\alpha$  weight fraction is  $(1-x)$ , assuming that the anhydrous trehalose consists only of these two phases. Thus, the total water uptake,  $b$ , can be accounted for in the following manner:

$$b = xa + (1-x)10.5 \quad (2)$$

where " $a$ " is the water (% w/w) sorbed by the amorphous fraction, and the water uptake required for anhydrate  $\rightarrow$  dihydrate transition is 10.5% w/w. At each experimental RH, while the value of  $b$  is obtained from the water sorption experiment, the water uptake behavior of freeze-dried amorphous trehalose at the same RH provides a measure of  $a$ . If these two values are known,  $x$  can be calculated using Eq. (3). The value  $(1-x)$  would be a measure of the weight fraction of the sample which has been converted to the dihydrate

$$x = \frac{b - 10.5}{a - 10.5} \quad (3)$$

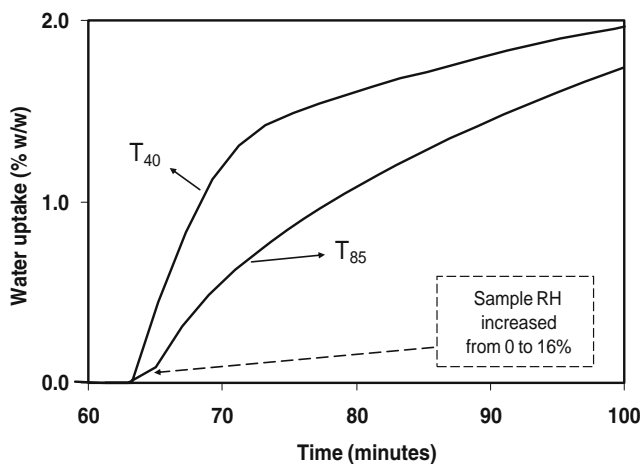


**Fig. 6.** The water sorption profiles of  $T_{40}$  and  $T_{85}$  at 16% RH in the automated vapor sorption balance (25°C). The initial sorption profile has been magnified in the inset.  $T_{40}$  shows a distinct biphasic sorption, the initial stage corresponding to the rapid incorporation of water into the highly ordered  $T_\alpha$  regions in the lattice to form  $T_H$ .

The implicit assumption is that the water sorption behavior of the amorphous fraction in the dehydrated trehalose is identical to that of the amorphous freeze-dried trehalose. This assumption may be reasonable as discussed earlier.

Table IV shows the extent of anhydrate  $\rightarrow$  dihydrate transition, as a function of RH. For the sake of discussion, let us assume that the anhydrous trehalose is composed of two distinct populations of crystalline  $T_\alpha$  and amorphous trehalose particles. We had earlier discussed that, at room temperature, the amorphous trehalose transformed to trehalose dihydrate only at RH  $\geq 50\%$ . Since these experiments were conducted either at 20 or at 30% RH, all the dihydrate formation should be due to transformation of the crystalline  $T_\alpha$ . The fraction of anhydrate converted to dihydrate should be the same at the two RH values. However, it is evident that there is a pronounced increase in the fraction of anhydrate transformed to dihydrate as the RH increased from 20 to 30%. We therefore believe that, in the anhydrous trehalose prepared by dehydration of trehalose dihydrate, there is a



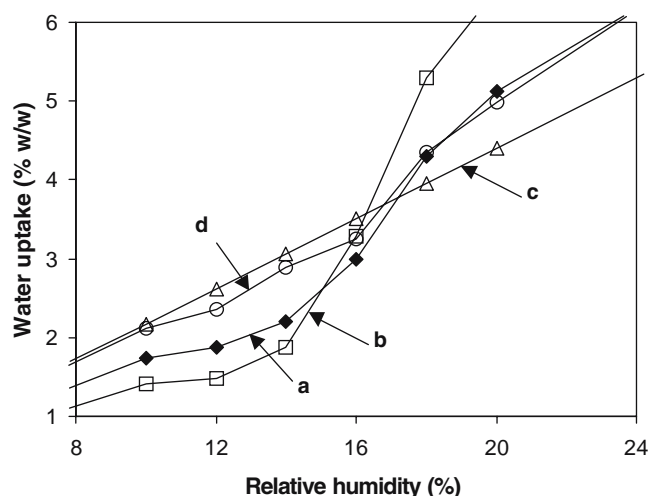


**Fig. 7.** Comparison of the water uptake behavior in the RH range of 10–20%: (a) Physical mixture (1:1 w/w) of  $T_{40}$  and  $T_{am}$ . (b)  $T_{40}$ . (c)  $T_{am}$ . (d)  $T_{85}$ .

continuum in lattice order ranging from highly crystalline  $T_{\alpha}$  to a completely disordered (i.e., amorphous) state. The higher the lattice order, lower the RH of transition to dihydrate.

We next compared the water sorption behavior of anhydrous trehalose samples with identical degree of crystallinity but prepared by different methods. Drying at 40°C and at 85°C yielded anhydrous trehalose with ~60 and ~30% crystallinity, respectively (by XRD; Table II). A second sample of ~30% crystallinity was prepared by physically mixing the  $T_{40}$  (~60% crystalline) with  $T_{am}$  prepared by freeze-drying (0% crystalline) in a 1:1 (w/w) ratio. It is evident from the water sorption profiles (Fig. 7) that the behavior of the physical mixture is a weighted average of the sorption behaviors of the  $T_{40}$  and  $T_{am}$ . Based on the two-state model of crystallinity, we would expect the sorption behavior of this mixture to be similar to that of  $T_{85}$ . Clearly, this is not the case. Though the degree of crystallinity of the two samples is nearly the same, their water sorption behavior showed pronounced differences. The physical mixture mirrors the water uptake behavior of  $T_{40}$  (e.g., significant conversion to the dihydrate at 16% RH) and was distinctly different from that of  $T_{85}$ . Thus the one-state model, according to which there is a continuum in lattice order, best describes the dehydrated sample.

Thus the effect of dehydration condition on the solid-state of the anhydrous trehalose can be summarized as follows. (i) The lower the temperature of dehydration, the more ordered the lattice. (ii) Dehydration resulted in an anhydrous material that exhibited a continuum in lattice disorder. With an increase in the temperature of dehydration, this continuum shifted towards higher degree of disorder.

Irrespective of the temperature, dehydration did not cause a change in particle morphology, and the prismatic habit of the  $T_H$  was retained in the anhydrous product (based on microscopic examination; data not shown). These results confirm earlier observations (16). The retention of the overall morphology of the particles suggests that the dehydration proceeds by a mechanism involving co-operative molecular movements leading to removal of the solvent via channels in the crystal lattice. This would result in a topotactic dehydra-

tion, which would also explain the reversible nature of the process (36). Moreover as also proposed by Petit and Coquerel, low temperature dehydration (“smoother route and slower rate of dehydration”) would maintain the system closer to thermodynamic equilibrium and the dehydration would proceed predominantly by a “co-operative reorganization” mechanism leading to transfer of structural information from the parent hydrate to the anhydrate. As the dehydration temperature is increased (“hard” condition; higher rates of water removal) the reorganization mechanism would change from “co-operative reorganization” towards “co-operative disorganization” leading to increased lattice disorder in the product phase. Thus the results obtained in the manuscript fit well into the co-operative dehydration model (36).

### Structure and Stability of $T_{\alpha}$

The physical properties of  $T_{\alpha}$  raise several interesting and pertinent questions about its structure and stability.  $T_{\alpha}$  melts at ~125°C which is ~90°C below the melting temperature of the room temperature stable polymorph,  $T_{\beta}$ . The reported enthalpy of fusion of 11.6 kJ/mole (33.9 J/g) of the highly crystalline ‘ $\alpha$ -polymorph’ is also substantially lower than the enthalpy of fusion of  $T_{\beta}$  of 52.6 kJ/mole (153.7 J/g) (14,25). Even substantially crystalline  $T_{\alpha}$  melts over a wide temperature range, a property not typically observed in highly crystalline solids including  $T_{\beta}$ . When the  $T_{\alpha}$  melt was cooled to room temperature, its properties were comparable to that of amorphous trehalose prepared by freeze-drying.  $T_{\alpha}$  has a stronger propensity to convert to trehalose dihydrate, than the amorphous anhydrate. While an amorphous anhydrate, because of its increased reactivity, is expected to transform to the hydrate at a lower water vapor pressure than its crystalline counterpart, this behavior of  $T_{\alpha}$  is unusual.

The difference in melting temperatures as well as the enthalpy of fusion make the  $\alpha$ - and  $\beta$ -forms an unusual polymorphic pair. Though the estimation of the free energy difference between the polymorphs, and the characterization of the type of polymorphic transition was outside the scope of this work, some general comments are in order. According to the heat of fusion rule formulated by Burger and Ramberger, “If the higher melting form has the lower heat of fusion the two forms are usually enantiotropic, otherwise they are monotropic.” (37) Based on this rule, the two forms seem to be related monotropically, with  $T_{\beta}$  being the stable form. When the  $T_{\alpha}$  melt was held at 150°, it resulted in the crystallization of  $T_{\beta}$ .

The physical stability of  $T_{\alpha}$  was assessed close to its melting temperature. Annealing of a partially crystalline solid, close to its melting temperature, usually facilitates crystallization. To test this possibility,  $T_{40}$  and  $T_{85}$  were annealed under different conditions. In the first case,  $T_{85}$  was annealed at 100°C for 3 or 10 h, cooled back and subjected to DSC (Fig. 8A). With an increase in the annealing time, the glass transition event (lower temperature shoulder in the DSC profile) became a separate endotherm due to the pronounced enthalpic recovery, while the higher temperature endotherm attributed to melting of  $T_{\alpha}$  did not change (Fig. 8A). In the second case,  $T_{40}$  or  $T_{85}$  were annealed at 110°C for 10 h, cooled back and then reheated (Fig. 8B). A higher temper-

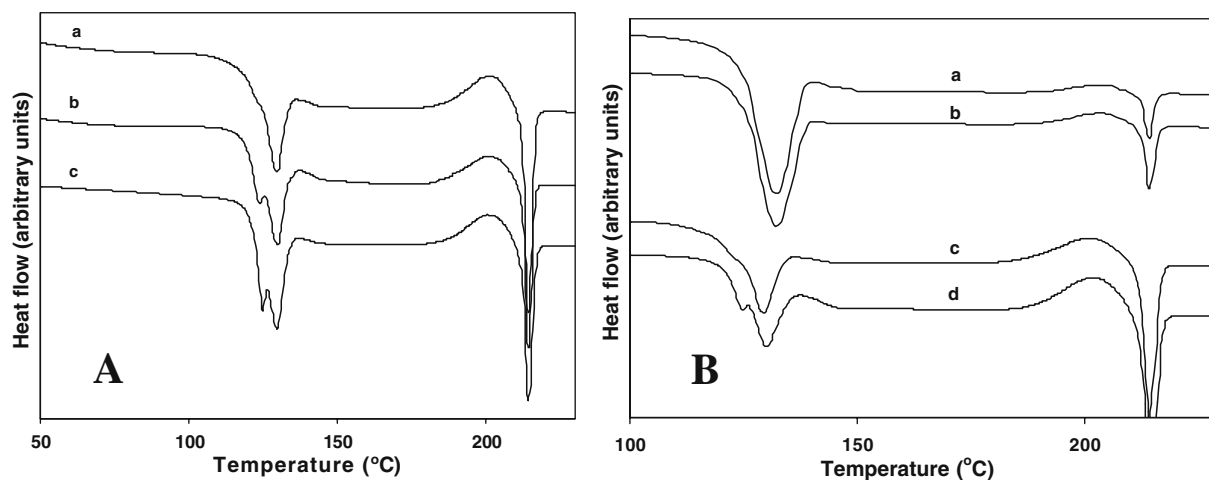


**Fig. 8.** (A) DSC heating profiles of  $T_{85}$  aged at  $100^{\circ}\text{C}$  for different time periods. (a) Unaged, (b) aged for 3 h, and (c) aged for 10 h. (B) DSC heating profiles of  $T_{40}$  (curves 'a' and 'b') and  $T_{85}$  (curves 'c' and 'd'). (a) and (c) were not annealed while (b) and (d) were annealed at  $110^{\circ}\text{C}$  for 10 h.

ature was chosen in this case to ensure adequate molecular mobility. The enthalpy of melting of these samples indicated that annealing did not increase the crystallinity of  $T_{\alpha}$ . Moreover, prolonged annealing also did not cause conversion to the stable  $T_{\beta}$ . In a separate set of experiments, prolonged annealing of amorphous trehalose in this temperature range also did not cause crystallization to  $T_{\alpha}$ . Thus,  $T_{\alpha}$  could not be prepared by any method usually known to crystallize amorphous materials nor could the crystallinity of the  $T_{\alpha}$  be increased by annealing.

Willart *et al.* observed that  $T_{\alpha}$  formation during dehydration occurred below a critical water removal rate of  $1.14 \times 10^{-5} \text{ ml min}^{-1} \text{ g m}^{-1}$ . At higher rates, the structure collapsed to yield an amorphous phase (27). It was also suggested that since the growth of  $T_{\alpha}$  during dehydration is restricted to the dehydrated zones within the lattice, it results in small coherent domains leading to broad X-ray diffraction peaks. (14) Our observations suggest that the disorder induced by water removal leads to X-ray peak broadening (Fig. 1). The angular range of the  $T_{\alpha}$  peaks substantially match the peak positions of the high intensity peaks in  $T_{\text{H}}$ . In crystalline hydrates, where dehydration can lead to an amorphous intermediate, the dehydration temperature is known to influence the solid-state of the anhydrous product phase. An increase in the dehydration temperature usually has the propensity to increase the crystallinity of the anhydrous product. For example, dehydration of carbamazepine dihydrate at temperatures  $\leq 30^{\circ}\text{C}$  yielded an amorphous anhydrate while higher temperatures yielded a partially or completely crystalline anhydrate (38,39). Interestingly, as the temperature of dehydration of trehalose dihydrate was increased, there was a progressive decrease in the crystallinity of the anhydrate. Trehalose is characterized by an unusually high glass transition temperature of  $117^{\circ}\text{C}$  and when dehydration occurred at much lower temperatures, the reduced mobility prevented complete lattice collapse. This inability of the lattice to collapse also conferred significant structural similarity between the anhydrous and the dihydrate phases. As the temperature of dehydration is

increased, the faster water loss coupled with enhanced molecular mobility increases the extent of lattice disorder.

#### $T_{\alpha}$ and its Relationship with $T_{\beta}$ and $T_{\text{am}}$

In light of the unique properties of  $T_{\alpha}$ , it will be instructive to compare its enthalpy with that of  $T_{\text{am}}$  and  $T_{\beta}$ . Aging of  $T_{\text{am}}$  (prepared by freeze-drying) at  $100^{\circ}\text{C}$  for 120 h, resulted in relaxation measured as an enthalpic recovery of 8.3 J/g, and an increase in  $T_{\text{g}}$  from  $117$  to  $124^{\circ}\text{C}$  (32). The magnitude of enthalpic recovery was comparable to the heat of fusion of partially crystalline  $T_{\alpha}$  (8.0 J/g) which was prepared by dehydration at  $85^{\circ}\text{C}$ . Thus the enthalpy state of partially crystalline  $T_{\alpha}$  was much closer to relaxed amorphous trehalose than to  $T_{\beta}$ .

On the other hand, the product obtained by dehydration at a lower temperature of  $40^{\circ}\text{C}$  exhibited a melting (onset at  $125^{\circ}\text{C}$ ) enthalpy of 20 J/g, reflecting its higher degree of lattice order and the consequent lower enthalpy state. While the self-limiting nature of the enthalpic relaxation process will make it impossible for a freeze-dried material to relax to this low enthalpy state in experimental time scales, it may be achievable by other routes.

Based on the unique behavior of  $T_{\alpha}$  it may be speculated that the lattice of  $T_{\alpha}$  produced by partial collapse of the trehalose dihydrate lattice is a kinetically stabilized ordered structure with substantial X-ray periodicity but negligible or very low lattice energy. When trehalose dihydrate is dehydrated at temperatures  $\ll$  glass transition of amorphous trehalose, though lattice disorder is induced, there is not enough mobility for complete collapse, resulting in a kinetically stable structure with residual order. This speculation is supported by the pronounced peak broadening in the XRD pattern of  $T_{\alpha}$ . Collapse of the  $T_{\alpha}$  structure very close to the glass transition of amorphous trehalose also lends support to this speculation.

The relationship between the structure in crystalline materials and the local 'structure' in corresponding organic glasses has been discussed by Shalaev and Zografis (40). In

this context, the trehalose system raises interesting questions. *Can the dehydrated phase retain a memory of the lattice order of the parent hydrate, with the extent of retention dependent on the disruptive effects of water removal? Is the lattice order in the dehydrated phase, which gives rise to the X-ray peaks and the DSC endotherm, retained only by virtue of the route of preparation and kinetic stabilization of the structure during preparation?*

### Significance

An increasing number of new chemical entities are poorly soluble in water. Amorphization is a widely investigated approach to enhance the aqueous solubility and potentially the bioavailability of such compounds. Retaining the material in the amorphous state, during processing and storage can be a challenge. On the other hand, highly crystalline solids can be unintentionally rendered amorphous, often partially, during processing. From a process or quality control perspective as well as that of final product performance, the quantification of crystallinity can be important. As mentioned earlier, the two-state model has formed the basis for quantification of crystallinity in pharmaceuticals. However, in several instances, it has been recognized that the model does not appropriately describe the lattice structure of partially crystalline pharmaceuticals (7,41,42). In case of trehalose, we have demonstrated the relevance and applicability of the one-state model to describe the partially ordered lattice. We believe that the one-state model is particularly relevant in case of disorder generated by processes such as dehydration and milling.

Trehalose synthesis, induced in organisms in response to desiccation stress, is believed to confer the ability to survive. Although the exact mechanism of this protective action is unknown, the ability of trehalose to form a rigid glassy structure and its ability to act as a hydrogen bonding water substitute are considered to be important factors in biopreservation (43). The stabilizing potential of trehalose has also been attributed to its ability to crystallize as a dihydrate (44). It was suggested that the rate of water uptake by the amorphous trehalose in  $T_{am} - T_{\alpha}$  mixtures was about an order of magnitude lower than that in pure amorphous trehalose (19). The ability of  $T_{\alpha}$  to take up water into the crystal lattice and convert to  $T_H$  is considered to be critical in its role in desiccation tolerance of anhydrobiotic organisms. The preferential uptake of water by  $T_{\alpha}$  would prevent plasticization (resulting in lowering of the  $T_g$ ) of the amorphous regions. Thus,  $T_{\alpha}$ , by acting as a water scavenger, would maintain the low mobility in the glassy phase and thereby aid in biopreservation (19). Our studies reveal that a decrease in the rate of water removal from the hydrate lattice resulted in an increased lattice order in the anhydrous product. Higher the lattice order in the anhydrate, lower the RH at which anhydrate  $\rightarrow$  hydrate transition was initiated. This reversibility is considered to be vital for desiccoprotection. While it is well known that  $T_{\alpha} \rightarrow T_H$  conversion occurs at a lower RH than  $T_{am} \rightarrow T_H$  transition, our study demonstrates that the RH at which  $T_{\alpha} \rightarrow T_H$  transition is initiated, is dictated by the extent of lattice order in the anhydrate. Extending this to the role of trehalose in

anhydrobiosis, the desiccation conditions might influence the extent of trehalose lattice order retained in desiccated organisms. This might affect the properties of the dehydrated trehalose and hence the nature and extent of protection afforded.

### CONCLUSIONS

The extent of lattice order in anhydrous trehalose was determined by the kinetics of water removal from trehalose dihydrate. The partially crystalline nature of anhydrous trehalose produced by dehydration could be described on a continuous scale of lattice order based on the one-state model of crystallinity.

### ACKNOWLEDGMENTS

We thank Dr. Evgenyi Y. Shalaev (Pfizer), Dr. Dushyant Varshney (Eli Lilly) and Dr. Lian Yu (University of Wisconsin—Madison) for their insightful comments and Dr. Lynne S. Taylor (Purdue University) for sharing her unpublished results and for the inspiring discussions. We dedicate this paper to Professor George Zografi. Though none of us formally trained with Professor George Zografi, we have learnt an immense amount from his published work.

### REFERENCES

1. H. G. Brittain (ed.), *Physical Characterization of Pharmaceutical Solids*, Marcel Dekker, New York, 1995.
2. J. K. Haleblan and W. McCrone. Pharmaceutical applications of polymorphism. *J. Pharm. Sci.* **58**:911–929 (1969).
3. D. Law, S. L. Krill, E. A. Schmitt, J. J. Fort, Y. Qiu, W. Wang, and W. R. Porter. Physicochemical considerations in the preparation of amorphous ritonavir-poly(ethylene glycol) 8000 solid dispersions. *J. Pharm. Sci.* **90**:1015–1025 (2001).
4. G. H. Ward and R. K. Schultz. Process-induced crystallinity changes in albuterol sulfate and its effect on powder physical stability. *Pharm. Res.* **12**:773–779 (1995).
5. M. D. Ticehurst, P. A. Basford, C. I. Dallman, T. M. Lukas, P. V. Marshall, G. Nichols, and D. Smith. Characterization of the influence of micronization on the crystallinity and physical stability of revatropate hydrobromide. *Int. J. Pharm.* **193**:247–259 (2000).
6. R. Huttenrauch. Molekulargalenik als grundlage moderner arzneiformung. *Acta Pharm. Technol.* **6**(Suppl.):55–127 (1978).
7. R. Suryanarayanan and A. G. Mitchell. Evaluation of two concepts of crystallinity using calcium gluceptate as a model compound. *Int. J. Pharm.* **24**:1–17 (1985).
8. M. J. Pikal. Impact of polymorphism on the quality of lyophilized products. In H. G. Brittain (ed.), *Polymorphism in Pharmaceutical Solids*, Marcel Dekker, 1999, pp. 395–419.
9. M. Ohta and G. Buckton. A study of the differences between two amorphous spray-dried samples of cefditoren pivoxil which exhibited different physical stabilities. *Int. J. Pharm.* **289**:31–38 (2005).
10. J. Han and R. Suryanarayanan. Influence of environmental conditions on the kinetics and mechanism of dehydration of carbamazepine dihydrate. *Pharm. Dev. Technol.* **3**:587–596 (1998).
11. S. Debnath and R. Suryanarayanan. Influence of processing-induced phase transformations on the dissolution of theophylline tablets. *AAPS PharmSciTech.* **5**(1):Article 8 (<http://www.aapspharmscitech.org>) (2004).

12. R. Surana, A. Pyne, and R. Suryanarayanan. Effect of preparation method on physical properties of amorphous trehalose. *Pharm. Res.* **21**:1167–1176 (2004).
13. J. F. Willart, A. De Gussemé, S. Hemon, G. Odou, F. Danede, and M. Descamps. Direct crystal to glass transformation of trehalose induced by ball milling. *Solid State Comm.* **119**:501–505 (2001).
14. J. F. Willart, A. De Gussemé, S. Hemon, M. Descamps, F. Leveiller, and A. Rameau. Vitrification and polymorphism of trehalose induced by dehydration of trehalose dihydrate. *J. Phys. Chem. B* **106**:3365–3370 (2002).
15. K. Akao, Y. Okubo, N. Asakawa, Y. Inoue, and M. Sakurai. Infrared spectroscopic study on the properties of the anhydrous form II of trehalose. Implications for the functional mechanism of trehalose as a biostabilizer. *Carbohydr. Res.* **334**:233–241 (2001).
16. S. P. Ding, J. Fan, J. L. Green, Q. Lu, E. Sanchez, and C. A. Angell. Vitrification of trehalose by water loss from its crystalline dihydrate. *J. Therm. Anal.* **47**:1391–1405 (1996).
17. T. Furuki, A. Kishi, and M. Sakurai. De- and rehydration behavior of  $\alpha,\alpha$ -trehalose dihydrate under humidity-controlled atmospheres. *Carbohydr. Res.* **340**:429–438 (2005).
18. H. Nagase, T. Endo, H. Ueda, and T. Nagai. Influence of dry conditions on dehydration of  $\alpha,\alpha$ -trehalose dihydrate. *STP Pharm. Sci.* **13**:269–275 (2003).
19. H. Nagase, T. Endo, H. Ueda, and M. Nakagaki. An anhydrous polymorphic form of trehalose. *Carbohydr. Res.* **337**:167–173 (2002).
20. F. Sussich, S. Bortoluzzi, and A. Cesaro. Trehalose dehydration under confined conditions. *Thermochim. Acta* **391**:137–150 (2002).
21. F. Sussich and A. Cesaro. Transitions and phenomenology of  $\alpha,\alpha$ -trehalose polymorphs inter-conversion. *J. Therm. Anal. Calorim.* **62**:757–768 (2000).
22. F. Sussich, F. Princivalle, and A. Cesaro. The interplay of the rate of water removal in the dehydration of  $\alpha,\alpha$ -trehalose. *Carbohydr. Res.* **322**:113–119 (1999).
23. F. Sussich, C. Skopec, J. Brady, and A. Cesaro. Reversible dehydration of trehalose and anhydrobiosis: from solution state to an exotic crystal? *Carbohydr. Res.* **334**:165–176 (2001).
24. F. Sussich, R. Urbani, A. Cesaro, F. Princivalle, and S. Bruckner. New crystalline and amorphous forms of trehalose. *Carbohydr. Lett.* **2**:403–408 (1997).
25. F. Sussich, R. Urbani, F. Princivalle, and A. Cesaro. Polymorphic amorphous and crystalline forms of trehalose. *J. Am. Chem. Soc.* **120**:7893–7899 (1998).
26. L. S. Taylor and P. York. Characterization of the phase transitions of trehalose dihydrate on heating and subsequent dehydration. *J. Pharm. Sci.* **87**:347–355 (1998).
27. J.F. Willart, F. Danede, A. Gussemé, M. Descamps, and C. Neves. Origin of the dual structural transformation of trehalose dihydrate upon dehydration. *J. Phys. Chem. B* **107**:11158–11162 (2003).
28. S.-Y. Lin and J.-L. Chien. *In vitro* simulation of solid–solid dehydration, rehydration, and solidification of trehalose dihydrate using thermal and vibrational spectroscopic techniques. *Pharm. Res.* **20**:1926–1931 (2003).
29. H. J. Reisener, H. R. Goldschmid, G. A. Ledingham, and A. S. Perlin. Formation of trehalose and polyols by wheat stem rust uredospores. *Can. J. Biochem. Physiol.* **40**:1248–1251 (1962).
30. Y. K.-I. Akao, Y. Okubo, Y. Inoue, and M. Sakurai. Supercritical CO<sub>2</sub> fluid extraction of crystal water from trehalose dihydrate. Efficient production of form II (Ta) phase. *Carbohydr. Res.* **337**:1729–1735 (2002).
31. J. Han and R. Suryanarayanan. A method for the rapid evaluation of the physical stability of pharmaceutical hydrates. *Thermochim. Acta* **329**:163–170 (1999).
32. R. Surana, A. Pyne, and R. Suryanarayanan. Effect of aging on the physical properties of amorphous trehalose. *Pharm. Res.* **21**:867–874 (2004).
33. P. H. Hermans and A. Weidinger. Quantitative X-ray investigations on the crystallinity of cellulose fibers. A background analysis. *J. App. Phys.* **19**:491–506 (1948).
34. H. A. Iglesias, J. Chirife, and M. P. Buera. Adsorption isotherm of amorphous trehalose. *J. Sci. Food Agric.* **75**:183–186 (1997).
35. M. G. Fakes, M. V. Dali, T. A. Haby, K. R. Morris, S. A. Varia, and A. T. M. Serajuddin. Moisture sorption behavior of selected bulking agents used in lyophilized products. *PDA J. Pharm. Sci. Tech.* **54**:144–149 (2000).
36. S. Petit and G. Coquerel. Mechanism of several solid–solid transformations between dihydrated and anhydrous copper(II) 8-hydroxyquinolates. Proposition for a unified model for the dehydration of molecular crystals. *Chem. Mater.* **8**:2247–2258 (1996).
37. A. Burger and R. Ramberger. On the polymorphism of pharmaceuticals and other molecular crystals. I. *Mikrochim. Acta* 259–271 (1979).
38. Y. Li, J. Han, G. Z. Zhang, D. J. W. Grant, and R. Suryanarayanan. *In situ* dehydration of carbamazepine dihydrate: a novel technique to prepare amorphous anhydrous carbamazepine. *Pharm. Dev. Technol.* **5**:257–266 (2000).
39. R. Surana, A. Pyne, and R. Suryanarayanan. Solid–vapor interactions: Influence of environmental conditions on the dehydration of carbamazepine dihydrate. *AAPS Pharm Sci Tech.* **4** (4):Article 68 (<http://www.aapspharmscitech.org>) (2003).
40. E. Shalaev and G. Zografi. The concept of ‘structure’ in amorphous solids from the perspective of the pharmaceutical sciences. In H. Levine (ed.), *Amorphous Food and Pharmaceutical Systems*, The Royal Society of Chemistry, Cambridge, UK, 2002, pp. 11–30.
41. N. Boutonnet-Fagegaltier, J. Menegotto, A. Lamure, H. Duplaa, A. Caron, C. Lacabanne, and M. Bauer. Molecular mobility study of amorphous and crystalline phases of a pharmaceutical product by thermally stimulated current spectrometry. *J. Pharm. Sci.* **91**:1548–1560 (2002).
42. M. Mosharraf and C. Nystroem. Apparent solubility of drugs in partially crystalline systems. *Drug Dev. Ind. Pharm.* **29**:603–622 (2003).
43. J. H. Crowe, J. F. Carpenter, and L. M. Crowe. The role of vitrification in anhydrobiosis. *Annu. Rev. Physiol.* **60**:73–103 (1998).
44. B. J. Aldous, A. D. Auffret, and F. Franks. The crystallization of hydrates from amorphous carbohydrates. *Cryo-Lett.* **16**:181–186 (1995).